Human neutrophil flavocytochrome b : structure and function
by Thomas Richard Foubert

A dissertation submitted in partial fulfillment of the requirements for the degree of Doctor of Philosophy in Microbiology
Montana State University

Abstract:
The catalytic core of the multi-subunit NADPH oxidase of neutrophils and other phagocytes is a hemoprotein known as flavocytochrome b558.. The structure of this protein has not been determined, thus preventing exploration of structure-function relationships that would provide a clearer picture of the molecular mechanisms that control oxidase function in vivo. The work presented herein summarizes the information that we obtained regarding 1) localization of the heme groups within the protein structure, and 2) identification of a possible allosteric mechanism of NADPH oxidase activation that incorporates changes in the molecular geometry of flavocytochrome b.

Detergent-solubilized flavocytochrome b was exposed to Staphylococcal V,8 protease for 1 hour. The digestion milieu was then fractionated by HPLC size-exclusion chromatography, resulting in isolation of a core fragment with a native heme absorbance spectrum, comprising two polypeptides of 60-66 and 17 kDa by SDS-PAGE. Sequence and immunoblot analyses of the deglycosylated polypeptide identified the polypeptide as the NH2-terminal 320 to 363 amino acid residues of gp91phox, and the NH2-terminal 169 to 171 amino acid residues of p22phox, providing the first direct evidence that the membrane-spanning regions of flavocytochrome b are responsible for heme ligation.

The anionic amphiphiles sodium- or lithium-dodecyl sulfate, and arachidonate (SDS, LD S, AA) initiate NADPH oxidase and proton channel activity in cell-free systems and intact neutrophils. To investigate whether these amphiphiles exert allosteric effects on flavocytochrome b, we developed a system using trisulfopyrenyl (Cascade Blue®, CCB)-labeled wheat germ agglutinin, or CCB-labeled monoclonal antibodies as extrinsic fluorescence probes for resonance energy transfer to the intrinsic hemes of detergent-solubilized and lipid-bound flavocytochrome b. In solution, flavocytochrome b complexed with both CCB conjugates and partially quenched the CCB fluorescence. Subsequent additions of SDS, LDS, or AA, but not the oxidase antagonist methyl ester of AA, to concentrations typical of cell-free oxidase assays caused a saturable, concentration-dependent relaxation of the fluorescence quenching. The relaxation effects were independent of complex dissociation, or alterations in the spectral properties of the chromophores, suggesting induction of a flavocytochrome b conformational change in which the proximity or orientation of the hemes have undergone significant movement relative to an extracellular reference point.

HUMAN NEUTROPHIL FLAVOCYTOCHROME *b*: STRUCTURE AND FUNCTION.

by

Thomas Richard Foubert

A dissertation submitted in partial fulfillment
of the requirements for the degree

of

Doctor of Philosophy

in

Microbiology

MONTANA STATE UNIVERSITY
Bozeman, Montana

January 2002

APPROVAL

of a dissertation submitted by

Thomas Richard Foubert

This dissertation has been read by each member of the thesis committee and has been found to be satisfactory regarding content, English usage, format, citations, bibliographic style, and consistency, and is ready for submission to the College of Graduate Studies.

Algirdas J. Jesaitis _____ (Signature) 1/17/02 Date

Approved for the Department of Microbiology

Clifford W. Bond _____ (Signature) 1/17/02 Date

Approved for the College of Graduate Studies

Bruce M. McLeod _____ (Signature) 1-17-02 Date

STATEMENT OF PERMISSION TO USE

In presenting this dissertation in partial fulfillment of the requirements for a doctoral degree at Montana State University, I agree that the library shall make it available to borrowers under rules of the library. I further agree that copying of this dissertation is allowable only for scholarly purposes, consistent with "fair use" as prescribed in the U.S. Copyright Law. Requests for extensive copying or reproduction to this dissertation should be referred to Bell & Howell Information and Learning, 300 North Zeeb Road, Ann Arbor, Michigan 48106, to whom I have granted "the exclusive right to reproduce and distribute my dissertation in and from microform along with the non-exclusive right to reproduce and distribute my abstract in any format in whole or in part."

Signature 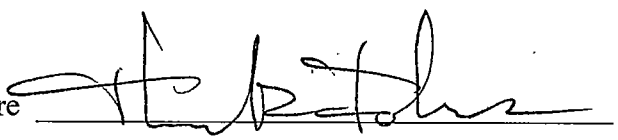

Date 4/17/02

TABLE OF CONTENTS

LIST OF TABLES

LIST OF FIGURES

Figure Page

ABSTRACT

The catalytic core of the multi-subunit NADPH oxidase of neutrophils and other phagocytes is a hemoprotein known as flavocytochrome b_{558}. The structure of this protein has not been determined, thus preventing exploration of structure-function relationships that would provide a clearer picture of the molecular mechanisms that control oxidase function *in vivo*. The work presented herein summarizes the information that we obtained regarding 1) localization of the heme groups within the protein structure, and 2) identification of a possible allosteric mechanism of NADPH oxidase activation that incorporates changes in the molecular geometry of flavocytochrome *b*.

Detergent-solubilized flavocytochrome *b* was exposed to *Staphylococcal* V8 protease for 1 hour. The digestion milieu was then fractionated by HPLC size-exclusion chromatography, resulting in isolation of a core fragment with a native heme absorbance spectrum, comprising two polypeptides of 60-66 and 17 kDa by SDS-PAGE. Sequence and immunoblot analyses of the deglycosylated polypeptide identified the polypeptide as the NH_2-terminal 320 to 363 amino acid residues of $gp91^{phox}$, and the NH_2-terminal 169 to 171 amino acid residues of $p22^{phox}$, providing the first direct evidence that the membrane-spanning regions of flavocytochrome *b* are responsible for heme ligation.

The anionic amphiphiles sodium- or lithium-dodecyl sulfate, and arachidonate (SDS, LDS, AA) initiate NADPH oxidase and proton channel activity in cell-free systems and intact neutrophils. To investigate whether these amphiphiles exert allosteric effects on flavocytochrome *b*, we developed a system using trisulfopyrenyl (Cascade Blue®, CCB)-labeled wheat germ agglutinin, or CCB-labeled monoclonal antibodies as extrinsic fluorescence probes for resonance energy transfer to the intrinsic hemes of detergent-solubilized and lipid-bound flavocytochrome *b*. In solution, flavocytochrome *b* complexed with both CCB conjugates and partially quenched the CCB fluorescence. Subsequent additions of SDS, LDS, or AA, but not the oxidase antagonist methyl ester of AA, to concentrations typical of cell-free oxidase assays caused a saturable, concentration-dependent relaxation of the fluorescence quenching. The relaxation effects were independent of complex dissociation, or alterations in the spectral properties of the chromophores, suggesting induction of a flavocytochrome *b* conformational change in which the proximity or orientation of the hemes have undergone significant movement relative to an extracellular reference point.

CHAPTER 1

INTRODUCTION

The NADPH Oxidase of Human Phagocytes

Neutrophils and other phagocytes of the host immune system play an important protective role by seeking out and destroying invading pathogenic organisms (1-4). Their ability to fulfill this task depends in large part on the function of a multi-subunit enzyme complex named the nicotinamide-adenine dinucleotide (NADPH) oxidase. Encounters between the phagocytes and any of several stimuli deriving from bacteria or damaged host cells results in activation of the oxidase. Once activated, the enzyme catalyzes the one-electron reduction of molecular oxygen to the highly energetic radical species superoxide anion (O_2^-) at the expense of intracellular NADPH. Subsequent complex chemical interactions between O_2^- and other constituents of the surrounding milieu produce a myriad of toxic oxygen species that are exploited in conjunction with other neutrophil cytoplasmic granule contents to destroy invading microorganisms (5-11).

Oxidase activation at the cellular level is usually receptor-mediated, involving several intracellular signaling pathways that culminate in assembly of the oxidase subunits at the neutrophil plasma membrane. *In vivo*, the oxidase comprises the cytosolic proteins, $p40^{phox}$, $p47^{phox}$, $p67^{phox}$, the membrane-associated Rac1 (or 2), or Rap1A (12-14), and a single transmembrane component, flavocytochrome b_{558} (6-9,15,16). Despite considerable investigation, the sequence of events that precede assembly of the oxidase

complex and the involvement of the individual subunits in controlling oxidase activity remain unclear. One consensus is that the presence of a minimum ensemble consisting of flavocytochrome *b*, p47^{phox}, and p67^{phox}, is absolutely necessary for normal oxidase activity *in vivo*. Deficiencies in any one of these proteins, arising from genetic lesions that either abolish expression or produce nonfunctional proteins, renders the oxidase catalytically inactive resulting in a clinical syndrome known as chronic granulomatous disease (CGD) (17-28). CGD is considered to be a rare disorder, affecting approximately one in 250,000-500,000 individuals, with no indication of racial preference. While the phagocytes of these individuals appear to otherwise function normally, certain organisms cannot be killed following phagocytosis. As a result, the phagocytes and their ingested pathogens accumulate, forming granulomatous lesions where the organisms thrive and are refractory to conventional treatment regimes. These granulomata, the histological hallmark of the disease, are found in lymph nodes, lungs, liver, bones and the subcutaneous tissues of the patients. Clinical symptoms may also present in the gastrointestinal tract as diarrhea, parianal abscesses, and obstructions due to granuloma formation. CGD is usually diagnosed in children under 2 years of age but has in some cases been recognized later due to the heterogeneous nature of the disease. The heterogeneity in clinical phenotypes is attributed to the immense complexity of the genetic lesions (for written reviews see (28,29), or see the X-CGD database at http://www.uta.fi/imt/bioinfo/CYBBbase/), and also the compensatory efficacy of redundant antimicrobial systems that can vary between individuals. Many of the

individuals suffering from this condition eventually succumb to the onslaught of infections and die within the first few years of life (21,24).

Although phagocytes perform a necessary function in host protection, misdirected or inappropriate generation of oxygen-derived radical species from these cells in otherwise healthy individuals contribute to a large number of disease processes such as atherosclerosis, Parkinson's disease, asthma, amyotrophic lateral sclerosis (ALS), adult respiratory distress syndrome (ARDS), and even aging (30-39). Phagocytes that emigrate to sites of injury play a significant part in mediating the initial phases of the inflammatory response by releasing a large number of compounds into the local environment, some of which are responsible for recruitment of other phagocytes and others that possess cytotoxic properties. The accumulative nature of this response sometimes results in non-specific damage to local tissues to an extent exceeding the initial insult, thus aggravating the injury (40-43)

Reactive oxygen metabolites appear to function as signaling molecules that are necessary for tissue neogenesis, fetal development, and apoptosis, hence implicating misdirected superoxide and other radical species in tumorogenesis (35,44-49). There is an emerging body of evidence that suggests that the oxidase also functions in the capacity of both an oxygen sensor (50-58) and a proton channel (49,59-72), though the latter function has recently been challenged (73). Additionally, homo- or orthologues of the oxidase subunits, primarily $gp91^{phox}$, continue to be identified in cells other than phagocytes (48,49,57,74-86). The prevalence of these homologues or the holoenzyme in such a variety of tissues suggests a multi-faceted biological role for these proteins.

Therefore, understanding the underlying molecular mechanisms that regulate oxidase or oxidase-related activity is of great importance, both for understanding cellular function, and for development of therapeutic strategies for control of inflammatory disease processes.

Human Neutrophil Flavocytochrome *b*

The central component of the NADPH oxidase is a transmembrane *b*-type cytochrome, flavocytochrome b_{558} (a.k.a. neutrophil cytochrome *b*, cytochrome b_{559}, flavocytochrome b_{-245}, and flavocytochrome *b*). The subscript 558 or 559 refers to the reduced α-band absorbance maximum (in nm) and the subscript –245 is an unconventional designation referring to the initially measured midpoint reduction potential (in mV) (87). The protein is a heterodimer (88) with a resting state 1:1 subunit stoichiometry (89-91) comprising a small non-glycosylated subunit, $p22^{phox}$, and an extensively glycosylated large subunit, $gp91^{phox}$ (the superscript *phox* is an abbreviation of *ph*agocyte *ox*idase, p and gp refer to protein or glycosylated protein, respectively). The primary sequence of both subunits have been deduced from cDNA, but there is no high-resolution structural information currently available for flavocytochrome *b*. Modeling studies suggest that the NH_2-terminal, roughly 60% of the protein contains several regions (two in $p22^{phox}$ and up to six in $gp91^{phox}$) that are likely to form membrane-spanning α-helical structures (17,18,20,92-95) (D. Baniulis, *et al.*, unpublished). The remaining C-terminal portion of the protein is relatively hydrophilic,

and predicted to reside on the cytosolic aspect of the neutrophil plasma membrane serving as a scaffold for assembly of the oxidase complex (10,96,97). Flavocytochrome *b* is the only membrane-spanning subunit of the oxidase, and therefore functions as the transmembrane conduit for electrons that are used to reduce extracellular molecular oxygen to O_2^- (6,97-101). Flavocytochrome *b* coordinates two (Taylor, *et al.*, unpublished), non-covalently bound heme moieties that are necessary elements of the electron transfer (94,102-105), and possibly proton conduction (106) pathways. Both FAD (107-121) and NADPH (113,118,122,123) are necessary for oxidase activity. Oxidase activity has been achieved *in vitro* in the absence of the cytosolic oxidase proteins by separate groups (124-128), and flavocytochrome *b* contains the necessary determinants of a complete electron transfer chain, i.e. NADPH $\rightarrow$ FAD $\rightarrow$ heme $\rightarrow$ O_2. Direct interactions that occur between flavocytochrome *b* and the other oxidase subunits, or between the oxidase subunits alone, have been revealed through the use of a variety of techniques (124,129-139). A consensus paradigm has emerged where flavocytochrome *b* is considered to be the only catalytic component of the oxidase, and oxidase activity is controlled by concerted interactions between flavocytochrome *b* and the other subunits. Investigation of these interactions has led to identification of the specific residues that define the protein-protein contact regions. These regions are therefore restricted to the intracellular aspect of the plasma membrane, and are also exposed to the cytoplasm, some only in the activated complex. Other studies have utilized antibodies, or antibodies in combination with other techniques, to determine both structural and functional aspects of the oxidase. Collectively, this information has contributed significantly to describing the

surface topology of some of the regions of the cytochrome. Although a substantial amount of information has been gathered, it remains unclear how these interactions confer oxidase activity *in vivo* or *in vitro*. The following sections summarize most of the currently available information that in some way contributes to defining the structure flavocytochrome *b*. The information is delineated by subunit, beginning at the NH_2-terminal regions of each of the subunits, with the initiation methionines designated as number 1. Although the initiation methionines do not appear to be present in the mature protein (88,140), they were included for consistency with the encoded sequences listed in the various protein data bases (e.g. NCBI accession numbers NM000101.1 and P04839 for $p22^{phox}$ and $gp91^{phox}$, respectively).

Structural and Functional Regions of $gp91^{phox}$.

Human $gp91^{phox}$ is encoded as a 570 amino acid residue protein with a predicted mass of 65.3 kDa based on primary sequence (20,95). The protein resolves by SDS-PAGE as a diffuse band of ~ 65 to 120 kDa (88) depending on the concentration of polyacrylamide used, and the cell type from which the protein was derived (141). The diffuse appearance is attributed to the extensively heterogeneous N-linked (88,142) glycosylation present at probably three of the five potential NXS/T sites, Asn^{131}, Asn^{148}, and Asn^{239} (93), thus restricting their location to the extracellular aspect of flavocytochrome *b*.

A number of studies suggest that specific regions of gp91^{phox} may bind one or more of the cytosolic subunits. Several studies have been conducted where the oxidase-inhibitory effects of peptides or antibodies were examined. Their effects were attributed to prevention of oxidase assembly based on the observation that they inhibit activation but not activity. While this perspective may be correct, an accurate definition of what is the "complex" in the active oxidase is still not fully clear at the present time and at least one study has suggested that some of the cytosolic subunits may interact with flavocytochrome *b* in a non-stoichiometric manner (143).

There is some experimental evidence suggesting that direct interactions occur between p67^{phox} and flavocytochrome *b* during oxidase activation. Paclet *et al.* inferred p67^{phox}-induced changes in flavocytochrome *b* structure on the basis of changes in liposome size during oxidase activation using atomic force microscopy (136). Two groups have been able to demonstrate *in vitro* oxidase activity in the presence of high concentrations of p67^{phox} and Rac, or Rac1 in the isoprenylated form, in the absence of p47^{phox} or anionic amphiphiles, suggesting p67^{phox} and possibly Rac1 interact directly with flavocytochrome *b* to regulate oxidase activity (139,144). Cross *et al.* conducted a kinetic study of activation *in vitro* and hypothesized that p67^{phox}, and possibly Rac2 interact in a catalytic fashion directly with flavocytochrome *b* to induce an active state geometry of the cytochrome (143).

Other investigations have suggested that gp91^{phox} binds to p67^{phox}, but the specific residues of either protein that are responsible for this putative interaction are still under investigation. Binding studies conducted by Dang *et al.* (145) showed that

phosphorylated p67^{phox} bound denatured gp91^{phox} on immunoblot. Dot blots of flavocytochrome *b* were also positive when probed with non-phosphorylated p67^{phox}. A GST-p67^{phox} fusion protein was also able to coprecipitate detergent-solubilized flavocytochrome *b*, and the interaction was significantly enhanced by the presence of either Rac1-GTPγS or GDPβS. In a separate study (146), a recombinant, bacterially-expressed C-terminal region of gp91^{phox} consisting of residues 307-570 showed weak superoxide dismutase (SOD) insensitive, NADPH-dependent nitroblue tetrazolium (NBT) reductase activity that was inhibitable by the oxidase inhibitor, diphenylene iodonium (DPI). The NADPH K_m for the truncated gp91^{phox} was similar to that of the native protein, and oxidase activity saturated at a 1:1 gp91^{phox}:FAD molar stoichiometry. This limited activity was increased slightly by addition of rac-1 and p67^{phox}, and doubled when truncated forms of p67^{phox} that retained the activation domain (147) were added. From these observations, the authors concluded that the interaction domain between flavocytochrome *b* and p67^{phox} was intact within this segment.

Oxidase inhibition studies conducted by Park *et al.* (148) utilized a series of peptides mimicking the predicted cytosolic domains of gp91^{phox}. Cytosolic subunit translocation assays with twelve different peptides showed that translocation of both p47^{phox} and p67^{phox} were affected with a corresponding reduction in oxidase activation. In particular, peptide 2, mimicking gp91^{phox} residues 87-100, was able to inhibit p67^{phox} translocation more extensively than p47^{phox} suggesting that the region might directly coordinate p67^{phox} – flavocytochrome *b* interactions.

In contrast to $p67^{phox}$-$gp91^{phox}$ interactions, considerable effort has been focused on determining the possible contact regions between $p47^{phox}$ and $gp91^{phox}$. Sequence analysis of an $X91^{+}$ CGD patient revealed a missense mutation predicting a $Asp^{500}\rightarrow Gly$ substitution in $gp91^{phox}$ (137). Neutrophils isolated from the patient exhibited severely attenuated translocation of both $p47^{phox}$ and $p67^{phox}$ to the membranes following PMA stimulation, and these same deficiencies were observed when the neutrophil membranes were tested in a cell-free assay. A synthetic peptide mimicking residues Phe^{491} to Gly^{504} of $gp91^{phox}$ was also able to inhibit oxidase activation in a cell-free system from normal neutrophils at an IC_{50} concentration of ~ 10 μM. Cell-free translocation assays indicated that both $p47^{phox}$ and $p67^{phox}$ did not associate with the membrane fraction, suggesting that the region was critical for cytosolic subunit binding.

Park *et al.* conducted oxidase inhibition and cytosolic subunit translocation assays using twelve different peptides corresponding to the predicted hydrophilic intracellular domains of $gp91^{phox}$ (148). Six of the twelve peptides designated 1, 2, 6, 7, 9, and 12 (corresponding to $gp91^{phox}$ residues 27-46, 87-100, 282-296, 304-321, 434-455, and 559-565 respectively) were shown to inhibit oxidase activation but not activity. Within this group, four of the peptides, 1, 2, 9, and 12 also partially inhibited translocation of the cytosolic subunits in a cell-free assay. Peptides 1 and 9 inhibited $p47^{phox}$ translocation to a greater extent than $p67^{phox}$ suggesting a possible direct interaction between $p47^{phox}$ and $gp91^{phox}$. The activation of the oxidase corresponded well with the extent of cytosolic subunit translocation with one exception, peptide 1. Interestingly, although peptide 1 (residues 27-46) only partially inhibited translocation of

the cytosolic subunits, it was highly effective in inhibiting oxidase activation (IC_{50} = 34 μM). A continuation of this study by the same group (149) revealed that truncated versions of peptide 9, corresponding to residues 418-435, and 441-450 of $gp91^{phox}$ (designated L418 and L441, respectively), also exerted inhibitory effects. Peptide L418 was able to inhibit oxidase activation *and* activity *in vitro* in the presence *or* absence of cytosol at an IC_{50} concentration of 10 μM. By testing scrambled and truncated versions of L418 in an *in vitro* superoxide assay, a minimum essential sequence was found, corresponding to residues ^{421}KSVWYK^{426} of $gp91^{phox}$ (designated L420). These tests further revealed that the terminal lysines as well as the tryptophan and tyrosine residues were critical for activity. Similar to L418, L420 was also shown to inhibit both oxidase activation and activity at an IC_{50} concentration of 35-40 μM. A kinetic study of *in vitro* oxidase inhibition indicated that the inhibitory effects of either peptide were uncompetitive with respect to NADPH binding, and with consistently lower overall K_M values in the presence of either peptide. These observations were interpreted to imply that L418 and L420 interacted directly with the flavocytochrome *b* and caused a structural perturbation that increased the affinity for NADPH. In contrast, peptide L441 exhibited irreversible inhibition at an IC_{50} concentration of ~ 58 μM suggesting a different inhibitory mechanism. The L418 and L420 peptides are the only ones reported to date that are able to inhibit both activation and activity of the oxidase.

A synthetic peptide corresponding to the C-terminal 551-570 residues of $gp91^{phox}$ (designated L_C) was shown to inhibit oxidase activation in a cell-free system from human neutrophils at an IC_{50} concentration of 4 μM in the presence of SDS (150). The peptide

was also shown to bind specifically to two proteins of 17 and 47 kDa by immunoblot using α-L_C antibodies, (probably $p47^{phox}$), but only after the cytosolic fractions had been incubated with SDS. Although this work was done prior to the designation of the 47 kDa protein as $p47^{phox}$, their results suggest a direct interaction between a 47 kDa protein and the extreme C-terminus of $gp91^{phox}$. This region of $gp91^{phox}$, as well as two others were also identified by DeLeo *et al.* in our laboratory by screening $p47^{phox}$ with a random-sequence peptide phage display library (129). Consensus sequences of phage peptides that bound $p47^{phox}$ identified three potential sites of interaction that corresponded to the regions, ^{87}STRVRRQL^{94}, ^{451}FEWFADLL^{458}, and ^{555}ESGPRGVHFIF^{565} of $gp91^{phox}$. Synthetic peptides corresponding to the ^{78}Phe-Leu^{94} and ^{452}Glu-Gln^{464} regions of $gp91^{phox}$ were also shown to inhibit oxidase activation *in vitro* at IC_{50} concentrations of 1 and 230 μM, respectively. To determine the regions of the ^{78}Phe-Leu^{94} that conferred the inhibitory effects, additional *in vitro* oxidation inhibition studies were conducted using peptides corresponding to $gp91^{phox}$ residues ^{78}Phe-Cys^{86} and ^{87}Cys-Leu^{94}. While the NH_2-terminal half of the ^{78}Phe-Leu^{94} peptide (^{78}Phe-Cys^{86}) exhibited no inhibitory effects at concentrations up to 500μM, the C-terminal portion of the ^{78}Phe-Leu^{94} (Cys^{87}-Leu^{94}) showed a similar efficacy to the full-length peptide ($IC_{50} \sim 3$ μM) indicating that the effector region was contained within the residues ^{87}CSTRVRRQL^{94}. These results suggested a direct interaction between $p47^{phox}$ and the residues ^{87}CSTRVRRQL^{94} of $gp91^{phox}$.

In a separate study, mutant forms of gp91^{phox} were generated by site-directed mutagenesis of human myeloid leukemia PLB-985 cells (151) targeting a similar domain of gp91^{phox} encompassing residues ^{87}CSTRVRRQLDRNLTFHK^{102}. The most profound effects on oxidase function were observed in the charge reversal Arg^{91}→Glu and Arg^{92}→Glu substitutions where membrane-translocation of the cytosolic oxidase proteins p47^{phox}, p67^{phox}, Rac1, and Rac2 were abolished. These observations suggested that p47^{phox} association with this region of gp91^{phox} and subsequent assembly of the oxidase were mediated by the residues Arg^{91} and Arg^{92}. This interaction site would necessarily be restricted to the intracellular aspect of the neutrophil membrane, and a separate modeling study further suggested a location near the intracytoplasmic face of the membrane (93).

Rotrosen *et al.* (152) was able to inhibit cell-free oxidase activation using rabbit polyclonal antibodies produced from a synthetic peptide CSNPRGVHFIFNKENF, that corresponded in part (underlined) to the extreme C-terminal ^{558}Pro-Phe^{570} residues of gp91^{phox}. The antibodies were shown to be positive for gp91^{phox} but only on the intracellular aspect of sheared neutrophil membrane patches indicating an intracellular location for the region. Six peptides mimicking gp91^{phox} residues 552-570, 559-570, 559-565, 552-558, 119-126 and 2-9 were tested for their ability to inhibit oxidase activity in both the broken cell superoxide assay, and electropermeabilized neutrophils. Only peptides 552-570, 559-570, and 559-565 had an inhibitory effect on oxidase activation, and none of the peptides affected oxidase activity after stimulation with arachidonate. Moreover, when these same peptides were allowed to diffuse into electroporated

neutrophils, they were able to inhibit both PMA- and fMLF-stimulated oxidase activation. These assays suggested that the inhibitory activity of the peptides was conferred by a minimum essential peptide sequence consisting of residues mimicking the ^{559}RGVHFIF^{565} residues of gp91^{phox}. The three peptides containing the ^{559}RGVHFIF^{565} sequence were also able to completely inhibit p47^{phox} phosphorylation in the cell-free assay suggesting that this region of flavocytochrome *b* may somehow modulate this activity. A separate kinetic study of oxidase activation in a cell-free system (153) derived from neutrophils of X91^{+} CGD patients lacking either p47^{phox} or p67^{phox}, revealed that the inhibitory effects of the ^{559}RGVHFIF^{565} peptide were exerted only when p47^{phox}-deficient cytosol was preincubated with AA and membranes that was later supplemented with exogenous p47^{phox}. The authors proposed that the peptide inhibited formation of a putative AA-dependent metastable activation intermediate that involved association of p47^{phox} with the membranes, possibly coordinated by the ^{559}RGVHFIF^{565} region of gp91^{phox}. Further studies suggested that the inhibitory effects of the peptide were conferred by the side chains of the Arg^{559}, Val^{561}, Ile^{564}, and both Phe^{563} and Phe^{565} residues (154).

The function of this region of gp91^{phox} was also explored *in situ* (155) with site-directed mutagenesis of gp91^{phox} expressed in an X-CGD PLB-985 cell line (156), targeting ^{559}RGVHFIF^{565} as well as adjacent residues. Mutant cells carrying single Ala substitutions at residues Arg^{559}, His^{562}, Phe^{563}, or Ile^{564}, and a double Ala substitution at Arg^{559} and Val^{561} had little effect on the maximal oxidase activity when compared wild-type PLB-985 cells. However, single point substitutions at Val^{561} with Ala, Thr, or Glu

resulted in a 2-4 fold reduction in superoxide generation, with the most dramatic effect due to the Val^{561}→Glu substitution. A single Ile^{564}→Ala substitution resulted in a 40% reduction in superoxide activity, and when mutated in tandem with a Phe^{565}→Val, all activity was lost. Single substitutions of Phe^{565} with either Ala or Asp caused a ~ 70 and 95% loss of activity, respectively, and a single Phe^{570}→Ala substitution caused a ~ 50% loss. These results were somewhat confounded by variable expression levels of flavocytochrome *b* as evidenced by immunoblot comparisons between $gp91^{phox}$ levels in cells expressing mutant $gp91^{phox}$ and wild-type PLB-985 cells. These variations in $gp91^{phox}$ expression levels were not taken into account for their functional comparisons, thus preventing accurate quantitation of relative activity. Deletion of the terminal 560-570 residues resulted in a complete loss of $gp91^{phox}$ expression suggesting that the region may be important for stable expression of flavocytochrome *b*.

A separate investigation (157) of the inhibitory effects of the ^{559}RGVHFIF^{565} peptide sequence was conducted utilizing a semi-recombinant reconstitution system consisting of isolated neutrophil plasma membranes and recombinant $p47^{phox}$, $p67^{phox}$ and Rac1. The peptide was found to inhibit AA-mediated plasma membrane translocation of both $p47^{phox}$ and $p67^{phox}$, and kinetic analyses suggested that the effects were non-competitive or mixed with respect to all of the cytosolic factors. The authors proposed that the effects of the peptide might be exerted by binding directly to and altering the conformation of flavocytochrome *b*. In contrast, a recent investigation by members of our laboratory (158) resulted in resolution of a three-dimensional structure of a peptide, corresponding to the C-terminal ^{551}SNSESGPRGVHFIFNKEN^{568} residues of $gp91^{phox}$,

bound to p47^{phox} using transferred nuclear Overhauser effect spectroscopy (Tr-NOESY) NMR. Correspondingly, the majority of the contact region was found to be contained within the segment ^{558}RGVHFIF^{564} indicating that this region of gp91^{phox} binds directly to p47^{phox}.

Collectively, the current data suggest that several regions of gp91^{phox} interact with the cytosolic subunits of the oxidase. These regions are therefore exposed to the neutrophil cytoplasm.

Structural and Functional Regions of p22^{phox}

Human p22^{phox} is a non-glycosylated (88), 192 amino acid residue protein (including the initiation methionine) with a predicted mass of 21.0 kDa based on primary sequence data (92). The presence of p22^{phox} is absolutely necessary for oxidase function *in vivo* as evidenced by p22^{phox} deficiencies that lead to a rare autosomal recessive form of CGD (19,28,159). p22^{phox} also appears to be necessary for stability of the flavocytochrome *b* heterodimer as the majority of CGD mutations that are confined to p22^{phox} also result in complete loss of gp91^{phox} (17,19,26,160-162).

Studies of interactions that occur between proteins that contain SH3 domains and their complimentary proline-rich target sites have identified a number of SH3-target sequence motifs including XPXXPPPΨXP (Ψ is a hydrophobic residue) (163) and PPRP (164), both of which are represented within the C-terminal ^{151}PPSNPPPRPP^{160} region of p22^{phox}. Several studies therefore, have been directed at determining if the tandem SH3

domains, that are present in both $p47^{phox}$ and $p67^{phox}$, might bind to this target region of $p22^{phox}$. Similar to $gp91^{phox}$, the primary focus of research has been directed towards interactions that occur between $p47^{phox}$ and $p22^{phox}$. However, a recent study conducted by Dahan *et al.*, utilizing the methodology of "peptide walking", suggested that $p67^{phox}$ might also bind $p22^{phox}$ (165). Ninety-one synthetic overlapping pentadecapeptides spanning the entire $p22^{phox}$ subunit were tested for their ability to either inhibit *in vitro* oxidase activation, or when immobilized, bind to the cytosolic subunits. They were able to identify three possible regions of $p22^{phox}$, namely, residues ^{81}Gly-Ala^{91}, ^{111}Thr-Ala^{115}, and ^{151}Pro-Pro^{160}, that appeared to coordinate interactions with $p67^{phox}$. They also identified $p22^{phox}$ residues ^{51}Leu-Ser^{63} and ^{151}Pro-Pro^{160} as binding sites for $p47^{phox}$, suggesting that both $p47^{phox}$ and $p67^{phox}$ target the same proline-rich C-terminal region of $p22^{phox}$.

Park *et al.* was able to inhibit *in vitro* oxidase activation using a 14 residue peptide corresponding to residues ^{82}PFTRNYYVRAVLHL^{95} of $p22^{phox}$ at an IC_{50} concentration of ~10 μM (166). Truncated versions of the peptide were also tested for their ability to inhibit oxidase activation, and a minimal sequence that retained inhibitory capacity (IC_{50} value lower than 50 μM) was found, consisting of residues ^{84}Thr-Leu^{93}. Single alanine replacements of the individual residues within another truncated peptide sequence, ^{83}Phe-Leu^{93}, with exception of Arg^{90} which was substituted with a glutamine, suggested that the central Tyr$^{87/88}$ and Val^{89} were the most crucial residues (~ 3-4-fold increase in IC_{50} concentrations), and to a lesser extent, Arg^{85} and Val^{92} (~ 2-fold increase IC_{50} concentrations). The oxidase inhibitory effects of this peptide are supported

experimentally by the work of Dahan *et al.* (165), who proposed that $p22^{phox}$ residues 81-91 might mediate $p67^{phox}$ binding.

Analysis of a CGD patient revealed normal expression levels of flavocytochrome *b* that showed no spectral abnormality, and normally functioning cytosol when tested *in vitro* with normal neutrophil membranes (167). Sequence analysis of the cDNA from the patient revealed a single-base substitution that predicted a nonconservative $Pro^{156} \rightarrow Gln$ substitution in one of the proline-rich C-terminal regions of $p22^{phox}$. Anti-peptide antibodies made from a synthetic peptide of the residues 153-164 of $p22^{phox}$ were shown to bind only to permeabilized neutrophils suggesting that epitope was located on the intracellular aspect of the neutrophil membrane. Further analyses of this mutation conducted by Leusen *et al.* (128), showed that membrane translocation of both $p47^{phox}$ and $p67^{phox}$ was severely attenuated in PMA-stimulated neutrophils isolated from the patient. In a cell-free assay, superoxide production was negligible when neutrophil membranes from the patient were tested with normal cytosol, and membrane translocation of $p47^{phox}$ and $p67^{phox}$ appeared to be completely abrogated. The neutrophil membranes of the patient exhibited cytosol-independent oxygen consumption, under conditions established by Koshkin and Pick (125,126), that was similar to control neutrophil membranes suggesting that NADPH and FAD binding were not affected. Although membrane translocation of both $p47^{phox}$ and $p67^{phox}$ were affected by the mutation, a peptide mimicking the putative SH3 binding domains of $p22^{phox}$ (residues 149-162), and another containing the $Pro^{156} \rightarrow Gln$ substitution, were both ineffective

(IC_{50} ~ 100 μM) at inhibiting oxidase activity when tested in a cell-free assay derived from normal neutrophils.

Nakanishi *et al.* (150) was able to substantially inhibit oxygen consumption in a cell-free assay activated with SDS by addition of a peptide mimetic (designated S_C) of the C-terminal 176-195 residues of $p22^{phox}$ (IC_{50} = 36μM). Additional experiments were conducted where cytosol and high concentrations of the peptide (100 μM) were incubated together, and then cross-linked with dimethyl 3,3'-dithiobis-propionimidate (DTBP). Immunoblots probed with α-S_C antibodies were positive for a 47 kDa protein that was probably $p47^{phox}$. DeLeo *et al.* (129) screened $p47^{phox}$ with a random-sequence peptide phage display library and found two consensus peptide sequences that corresponded to the putative SH3 binding regions, residues 156-160 and 177-183 of $p22^{phox}$. In contrast to the results obtained by Nakanishi *et al.* (150), a peptide mimicking the same C-terminal 176-195 residues of $p22^{phox}$ was shown to be a poor inhibitor of oxidase activation *in vitro* (IC_{50} ~ 500μM).

In a tour de force, Leto *et al.* (168) also conducted a study aimed at identifying the oxidase protein target sites of the SH3 binding domains of $p47^{phox}$ and $p67^{phox}$. GST-fusion proteins were constructed with short peptide sequences corresponding to the SH3 domains of $p47^{phox}$ ($p47^{phox}/SH3_{A-B}$, residues 151-284; $p47^{phox}/SH3_A$, and $/SH3_B$, residues 151-214 and 227-284, respectively) and $p67^{phox}$ ($p67^{phox}/SH3_A$ and $/SH3_B$, residues 241-304 and 458-526, respectively). Two additional constructs were made, one with GST fused to the cytoplasmic domain of $p22^{phox}$ (GST-$p22^{phox}$)(residues 127-195), and another with the same residues but containing a Pro^{156}→Gln substitution (GST-$p22^{phox}$Δ). These

$p22^{phox}$ fusion proteins were then subjected to SDS-PAGE, transferred to nitrocellulose, and probed with affinity purified, biotinylated $p47^{phox}$ and $p67^{phox}$ SH3 fusion proteins. Under these conditions, the $p47^{phox}/SH3_{A-B}$ probe bound to GST-$p22^{phox}$ and $p47^{phox}$, but not GST-$p22^{phox}\Delta$ or $p67^{phox}$. Probing with $p47^{phox}/SH3_A$ produced only weak signal, but probing with $p47^{phox}$ $SH3_B$ showed strong binding to both GST-$p22^{phox}$ and GST-$p22^{phox}\Delta$ suggesting that the specificity of the interaction was compromised in the absence of both SH3 domains. Conversely, probing with either of the $p67^{phox}$ constructs produced only weak signal suggesting a lower affinity for the C-terminal region of $p22^{phox}$, or possibly that both $p67^{phox}$ SH3 domains were necessary for efficient binding. Several peptides representing the proline-rich regions of either $p22^{phox}$ (residues 149-162, or 149-162 $Pro^{156}\rightarrow Gln$, and 176-195) or $p47^{phox}$ (residues 70-83, 338-351, and 358-371) were tested for their ability to inhibit binding interactions on the immunoblots. Peptide $p22^{phox}$ 149-162 was the only effective inhibitor of the $p22^{phox}$-$p47^{phox}$ binding interaction. Peptide $p22^{phox}$ 176-195 was unable to inhibit binding, as was the 149-162 $Pro^{156}\rightarrow Gln$ peptide, thus corroborating the *in vitro* functional results of both DeLeo *et al.* (129) and Leusen *et al.* (128), and also confirming the biochemical effects of the CGD mutation (167). Further experiments using EBV-transformed $p22^{phox}$ deficient B-cells expressing either wt $p22^{phox}$ or $p22^{phox}$ $Pro^{156}\rightarrow Gln$ (168) showed that oxidase activity could only be rescued by transfection with wt $p22^{phox}$. Transfection of a K562 erythroleukemia cell line with the same constructs demonstrated that translocation of $p47^{phox}$ was completely abolished by the $Pro^{156}\rightarrow Gln$ substitution, and also that $p47^{phox}$ translocation occurred in the absence of $gp91^{phox}$.

Sumimoto *et al.* (169) performed similar experiments with GST-fusion protein constructs to specifically examine the interactions between the SH3 domains of $p47^{phox}$ and the C-terminal proline-rich region of $p22^{phox}$. A GST-fusion protein containing the SH3 domains (residues 154-285) of $p47^{phox}$ (GST-$p47^{phox}$-SH3) was shown to inhibit superoxide activity in a cell-free assay, activated with either 50 μM AA or 100 μM SDS, at an IC_{50} concentration of ~ 20 nM. GST-fusion proteins were also expressed that contained the residues 132-195, 145-170, 151-160 of $p22^{phox}$, and two additional ones containing residues 132-195, and 151-160, but including the known CGD mutation Pro^{156}→Gln (167). These GST-$p22^{phox}$ protein constructs were subjected to SDS-PAGE, transferred to nitrocellulose, and then probed with biotinylated GST-$p47^{phox}$-SH3. GST-$p47^{phox}$-SH3 bound only GST-$p22^{phox}$ proteins that were lacking the Pro^{156}→Gln substitution, with the highest affinity interaction observed between GST-$p47^{phox}$-SH3 and GST-$p22^{phox}$-(132-195). Although GST-$p22^{phox}$-(151-160) contained the proline-rich, putative SH3 target sequence, binding to this region by GST-$p47^{phox}$-SH3 was considerably diminished, suggesting that the structure of the SH3 target region was compromised, or possibly that SH3-mediated binding is only partly responsible for the interprotein coordination.

A later study conducted by the same group (170) investigated which of the $p47^{phox}$ SH3 domains bound to $p22^{phox}$, and also which of the specific proline sequences of $p22^{phox}$ was responsible for the interaction. Using the same system, they expressed GST-$p47^{phox}$ fusion proteins containing full length $p47^{phox}$ ($p47^{phox}$-F, residues 1-390), $p47^{phox}$ SH3(N) (residues 154-219, and 154-219 with a Trp^{193}→Arg substitution), $p47^{phox}$

SH3(C) (residues 223-286), and p47^{phox}(SH3)$_2$ (residues 154-286). GST-p22^{phox} fusion proteins were also expressed that contained residues 132-195, 132-195 with Pro^{156}→Gln substitution, 132-150, 132-170, 145-170, 145-195, and 163-195. Immunoblots of the GST-p22^{phox}-132-195 fusion protein were probed first with the various GST-p47^{phox} fusion proteins, and then an α-GST monoclonal antibody. Strong binding was evident between p47^{phox} SH3(N) and GST-p22^{phox}-132-195, but was completely abolished with GST-p22^{phox}-132-195 Pro^{156}→Gln indicating that the region represented at least one target for the SH3-mediated interactions. The mutant p47^{phox} SH3(N)-(154-219, Trp^{193}→Arg) also failed to bind the GST-p22^{phox}-132-195 suggesting that p47^{phox} SH3(N) binds p22^{phox} in a manner common among SH3 binding proteins (171,172) where a tryptophan residue interacts directly with a proline. Immunoblots of GST-fusion p22^{phox} proteins probed with p47^{phox}-SH3(N) showed strong binding to GST-fusion p22^{phox} proteins that contained the stretch ^{152}PSNPPPRPP^{162}. In contrast, GST-fusion p22^{phox} proteins that lacked this stretch (residues 132-150, and 163-195) did not interact with p47^{phox}-SH3(N) indicating that the ^{152}PSNPPPRPP^{162} region was the target for the SH3 regions of p47^{phox}. These results were confirmed *in vivo* using two separate yeast two-hybrid systems where productive interactions were observed only in cells that coexpressed both p22^{phox}-(132-195) and p47^{phox}(SH3)$_2$ (residues 154-286). GST-p22^{phox}-132-195 immobilized on a biosensor tip in a resonance mirror system (173-175) was also shown to directly bind GST-p47^{phox} SH3(N) or GST-p47^{phox}(SH3)$_2$ (respective K_ds of 0.34 and 0.36μM), but not GST-p47^{phox} SH3(N) containing the Trp^{193}→Arg substitution, or GST-p47^{phox}-SH3(C). Lastly, GST-p47^{phox}-F was able to reconstitute full activity in a

cell-free superoxide assay in the presence of anionic activators, whereas GST-p47^{phox}-F containing the Trp^{193}→Arg substitution was inactive. These findings suggest that the SH3(N) domain of p47^{phox} (residues 154-219) binds specifically to the C-terminal proline-rich region (residues ^{152}PSNPPPRPP^{162}) of p22^{phox}.

In similar experiments (176), a truncated form of p47^{phox} that was lacking the C-terminal Arg/Lys regions (p47^{phox}-ΔC, residues 1-286) was precipitated by a maltose binding protein (MBP) fusion construct containing p22^{phox} residues 132-195 (MBP-22-C), but not by MBP-22-C carrying the Pro^{156}→Gln substitution. MBP-22-C was also able to precipitate full-length GST-p47^{phox}-F (residues 1-390) substitution mutants containing Pro$^{229/300}$→Gln, Arg$^{301/302}$→Glu, and Ser$^{303/304/328}$→Asp, but not wt GST-p47^{phox}-F, or p47^{phox}-F substitution mutants carrying Ser^{328}→Asp, or Ser$^{303/304}$→Asp replacements. To further test the hypothesis that disruption of the intramolecular interactions within p47^{phox} were necessary to promote accessibility of the SH3 domain to p22^{phox}, they conducted *in vivo* experiments using a Y190 yeast two-hybrid system. Positive binding interactions were observed only in cells that were co-transformed with p22^{phox}-C and either p47^{phox}-ΔC, or p47^{phox}-(1-302), but not wt p47^{phox}-F. In the same system, p47^{phox}-F double mutants with Pro$^{299/300}$→Gln, or Arg$^{301/302}$→Glu substitutions, were both able to bind p22^{phox}-C. However, under the same conditions, a p47^{phox}-F double mutant with aspartate substitutions at Ser$^{303/304}$→Asp failed to interact with p22^{phox}-C, thus consistent with observations from their precipitation experiments. C-terminally truncated versions of p47^{phox} (residues 1-327 or 1-340), both with the double

$Ser^{303/304}$→Asp substitution were also tested in the yeast two-hybrid assay. The $p47^{phox}$-(1-327), $Ser^{303/304}$→Asp was able to bind $p22^{phox}$-C, but inclusion of a third Ser^{328}→Asp substitution within the $p47^{phox}$-(1-340) truncated mutant, and also into the $p47^{phox}$-F conferred positive binding activity, whereas the single Ser^{328}→Asp substitution was inactive. Additional $p47^{phox}$-F substitution mutants were tested, where serines 303, 304, 315, 320, 328, 345, 348, 359, 370, and 379 were all simultaneously replaced with aspartate, or all but serines 303, 304, or 328 were replaced. Only the mutant $p47^{phox}$-F that contained simultaneous aspartate substitutions at serines 303, 304, and 328 could bind $p22^{phox}$-C, suggesting that these residues were critical for intramolecular masking of the SH3 domain that binds $p22^{phox}$.

Since the GST-$p47^{phox}$-ΔC mutant was previously shown able to initiate a limited amount of amphiphile-independent superoxide production *in vitro* (177,178), GST-$p47^{phox}$-F proteins, wt or substitution mutants ($Pro^{299/300}$→Gln, $Arg^{301/302}$→Glu, $Ser^{303/304}$→Asp, Ser^{328}→Asp, $Ser^{303/304/328}$→Asp), were also tested for their ability to reconstitute superoxide activity *in vitro* in the presence or absence of SDS. Oxidase activation using wt GST-$p47^{phox}$-F was absolutely dependent on the presence of SDS. In the absence of SDS, GST-$p47^{phox}$-F mutants $Pro^{299/300}$→Gln, $Arg^{301/302}$→Glu, and $Ser^{303/304/328}$→Asp were all capable of reconstituting *in vitro* oxidase activity at ~ 50% of the amphiphile-activated system, but at a ~ 5-8 fold higher concentration relative to GST-$p47^{phox}$-ΔC. The triply mutated GST-$p47^{phox}$ ($Ser^{303/304/328}$→Asp) was the least active, requiring the highest concentration (~ 400 nM) to achieve oxidase activity close to

$p47^{phox}$-ΔC (~ 50 nM). All of the mutant GST-$p47^{phox}$ tested showed similar activity in the presence of SDS. The ability of the different mutants to reconstitute oxidase activation *in vitro* corresponded identically to their ability to bind $p22^{phox}$ shown in their previous experiments. These results suggest that the rate-limiting step in oxidase activation *in vitro* in their system was dependent on $p47^{phox}$ binding to $p22^{phox}$. The effects of these $p47^{phox}$ mutations were further investigated *in vivo* using transfected K562 cells, where serines 303, 304, and 328 were replaced with alanine, a residue that cannot be phosphorylated. Cells transfected with wt $p47^{phox}$-F were capable of full oxidase activity, whereas cells expressing mutant $p47^{phox}$-F containing either Ser^{328}→Ala or $Ser^{303/304}$→Ala substitutions showed very little oxidase activity even though similar amounts of $p47^{phox}$ were expressed. Collectively, these results suggest that simultaneous phosphorylation of $p47^{phox}$ serines 303, 304, and 328 is necessary for disruption of intramolecular binding interactions within $p47^{phox}$. Once disrupted, the SH3 domains of $p47^{phox}$ are unmasked, thereby allowing interaction with the C-terminal regions of $p22^{phox}$ and subsequent activation of the oxidase.

Huang and Kleinberg (132) used a *Saccharomyces cerevisiae* yeast two-hybrid system to study the interactions between the SH3 ($p47^{phox}$-$NTSH3_{A-B}$, residues 1-285; $p47^{phox}$-$SH3_{A-B}$, residues 154-285; $p47^{phox}$-$SH3_A$, and -$SH3_B$, residues 146-228 and 222-285, respectively) and the Arg/Lys (residues 286-351) domains of $p47^{phox}$, with the C-terminal region of $p22^{phox}$ ($p22^{phox}$-CT, residues 135-195). Again, the role of the Pro^{156} of $p22^{phox}$ was investigated by incorporating a Pro^{156}→Gln substitution into the C-terminal region of $p22^{phox}$ ($p22^{phox}$-*CT). Additionally, full length $p47^{phox}$, either wt or mutated,

were expressed as either B42 or LexA activation domain fusion proteins in a yeast two-hybrid system. In the yeast two-hybrid binding assay, $p47^{phox}$-$SH3_A$ and $p47^{phox}$-$SH3_{A-B}$, but not $p47^{phox}$-$SH3_B$, bound $p22^{phox}$-CT, and none of the $p47^{phox}$ constructs bound to $p22^{phox}$-*CT. Unexpectedly, coprecipitation of $p47^{phox}$-$SH3_{A-B}$ by immobilized GST-$p22^{phox}$-CT, could also be blocked by synthetic $p47^{phox}$ Arg/Lys domain peptides corresponding to residues 301-320 and 314-335 even though these peptide regions did not bind to $p22^{phox}$-CT in the yeast two-hybrid assay. These peptide regions, when expressed as GST-$p47^{phox}$ fusion proteins, also failed to coprecipitate GST-$p22^{phox}$-CT. Further investigation, using the yeast two-hybrid system, showed that wt $p47^{phox}$ did not interact with $p22^{phox}$-CT. To investigate whether $p47^{phox}$ Arg/Lys domain binding to the $SH3_{AB}$ domain could be reversed by conditions mimicking phosphorylation, or anionic amphiphile interaction, aspartate or alanine substitutions were incorporated within the Arg/Lys domain of wt $p47^{phox}$ at Ser^{310} and Ser^{328}. Serine replacement, either separately or in tandem, with alanine or aspartate was intended to mimic neutral or negative charge, respectively. Positive binding interactions with $p22^{phox}$-CT, but not $p22^{phox}$-*CT, were observed for the both single and double Ser^{328}→Asp substitutions, and also with the single Ser^{310}→Ala substitution. These results indicated that a single, negatively-charged residue within the Arg/Lys domain was sufficient to disrupt the intraprotein binding between the Arg/Lys and the $SH3_{AB}$ domains of $p47^{phox}$, and that the interaction might be stabilized by the hydroxyl side group of Ser^{310}. Superoxide generation *in vitro* with wt $p47^{phox}$ required addition of arachidonate, whereas similar amounts of activity were achieved with $p47^{phox}$-$SH3_{AB}$ that showed no dependence on arachidonate. Their results

suggested that the $p47^{phox}$ Arg/Lys domains interact preferentially with the SH3 domains of $p47^{phox}$, and block the $SH3_A$ domain of $p47^{phox}$ from binding the C-terminal, proline-rich region of $p22^{phox}$. They hypothesized that, *in vivo*, incorporation of a negative charge by serine phosphorylation within the Arg/Lys domain of $p47^{phox}$ could disrupt intramolecular interactions with the SH3 domains, thereby enabling binding between $SH3_A$ and the C-terminal proline-rich region of $p22^{phox}$. In support of this hypothesis, expression of a double mutant $p47^{phox}$ containing alanine substitutions at serines 303 and 304 was unable to restore normal oxidase activity in an EBV-transformed $p47^{phox}$-defficient cell line (179). However, transfection with a double mutant $p47^{phox}$ containing either glutamate or lysine substitutions of the same serines was able to rescue oxidase activity, thus contrasting the results of Ago *et al.* (176).

Interactions Between $gp91^{phox}$ and $p22^{phox}$

The specific residues that form the interfacial contact region between $p22^{phox}$ and $gp91^{phox}$ have not been identified. Recent proteolysis experiments conducted by our group (140) resulted in isolation of a spectrally stable core polypeptide comprising the NH_2-terminal 320 to 363 amino acid residues of $gp91^{phox}$, and the NH2-terminal 169 to 171 amino acid residues of $p22^{phox}$. The overall stability of the polypeptide, as evidenced by retention of a native Soret absorbance spectrum, suggested that the $gp91^{phox}$-$p22^{phox}$ interprotein contact residues were contained within this core polypeptide.

Cofactor Binding Regions of Flavocytochrome *b*.

NADPH

Early attempts at identification of the NADPH-binding component(s) of the oxidase using affinity labeling with NADPH analogues produced conflicting reports of membrane bound proteins of 66 (180,181) and 32 kDa (182), and one 66 kDa cytosolic protein (183) that may have been $p67^{phox}$ (184,185). The first compelling evidence that $gp91^{phox}$ could bind NADPH was provided by Segal and coworkers using the NADPH analogue, ^{32}P-labeled 2-azido-NADP (114). Labeling with this derivative was positive for $gp91^{phox}$ derived from normal neutrophils, but negative when tested against neutrophil membranes of $X91^0$ CGD patients. Confirmation of NADPH binding to $gp91^{phox}$ was provided by later experiments conducted by separate groups using other NADPH analogues such as the tritiated NADPH derivative, [4-[N-(4-azido-2-nitrophenyl)[^{3}H]amino]butyryl]NADPH ([^{3}H]azido-NADPH) (122), and also by reduction of the schiff base formed between an NADPH analogue, pyridoxal-5′-diphospho-5′-adenosine (186), and $gp91^{phox}$ with Na[^{3}H]BH_4 (123). Han *et al.*, using a recombinant bacterial expression system to produce truncated forms of $gp91^{phox}$, was able to further localize the NADPH binding domain to the C-terminal 306-569 amino acid residues of the protein (146).

Details of the specific gp91^{phox} residues that might coordinate NADPH have been inferred by sequence comparison to NADPH binding domains of other flavoproteins such as porcine and human NADH-cytochrome *b*5 reductase, spinach ferredoxin-NADP+ reductase (FNR), ferric reductase of *Saccharomyces cerevisiae* (FRE1), rat nitric oxide synthase (NOS), NADPH-cytochrome *P*450 reductase (CPR) from *Bacillus megaterium* and rat, tomato NADH-nitrate reductase, NADPH-sulfite reductase, and the human gp91^{phox} homologue, p65^{phox} (113-115,124,187-197). A consensus NADPH-binding motif was found, composed of a glycine-rich stretch, GXGXGXXPF, in tandem with a separate CG couplet. This motif is present in the C-terminal regions of gp91^{phox} corresponding to residues ^{408}GAGIGVTPF^{416}, and ^{534}VFXCGP^{539}.

Several CGD case studies provide indirect support for these regions as NADPH binding sites. An X91^{+} CGD case was found to be caused by a single Leu^{546}→Pro substitution in gp91^{phox} (198). The authors proposed that inclusion of a Pro residue could severely perturb the putative α-helical structure that was predicted for this region of gp91^{phox} (197), and thus affect NADPH binding. In a separate X91^{+} CGD case, arising from a single Pro^{415}→His point mutation in gp91^{phox} (199), the physicochemical properties of the flavocytochrome *b* heme from the patient appeared normal with respect to absorbance spectrum, redox potential and CO binding (200). Although normal amounts of flavocytochrome *b* were present in the neutrophil membranes of this patient, labeling with the NADPH analogue ^{32}P-labeled 2-azido-NADP was abolished (114). The same mutation was found in another CGD patient (201). Biochemical analyses of neutrophils from the patient showed that the flavocytochrome *b* was able to bind normal